JOURNAL OF THERMOPHYSICS AND HEAT TRANSFER
Vol. 10, No. 2, April–June 1996

Measurement of Catalytic Recombination Coefficients on Quartz Using Laser-Induced Fluorescence

Joan B. Pallix*
NASA Ames Research Center, Moffett Field, California 94035
and
Richard A. Copeland†
SRI International, Menlo Park, California 94025

Advanced laser-based diagnostics have been developed to examine catalytic effects and atom/surface interactions on thermal protection materials. This study establishes the feasibility of using two-photon laser-induced fluorescence for detection of O and N atom loss in a diffusion tube to measure surface catalytic activity. The experimental apparatus is versatile in that it allows fluorescence detection to be used for measuring species selective recombination coefficients and for performing diffusion tube and microwave discharge diagnostics. Many of the potential sources of error in measuring atom recombination coefficients by this method have been identified and taken into account. These include scattered light, detector saturation, sample surface cleanliness, reactor design, gas pressure and composition, and selectivity of the laser probe. Recombination coefficients and their associated errors are reported for N and O atoms on a quartz surface at room temperature.

Nomenclature

D = diffusion coefficient
F = surface roughness factor
f_L = laser fluence
I = fluorescence intensity
J = spin–orbit splitting level
M = atomic mass
P = reactor pressure
R = ideal gas constant
r = inside radius of diffusion tube
T = reactor temperature
v = average atomic speed, $(8RT/\pi M)^{1/2}$
X = distance from center of microwave discharge cavity
γ = atom recombination coefficient
μ = slope of atom decay curves, $\ell n(I)$ vs X/r

Introduction

TO develop more effective advanced thermal protection materials for spacecraft, an understanding of the behavior of these materials under atmospheric entry heating conditions is essential. It has been shown that, during Earth entry, heterogeneous atom recombination with an exothermic heat of reaction can account for a significant fraction of the surface heating rate.[1,2] There have been numerous experimental investigations of this phenomenon over the past 25 years. Although some benchtop laboratory studies have been made, most of the catalytic recombination data on spacecraft materials results from arcjet testing at high enthalpy in dissociated airflows. These arcjet studies provide relative catalytic efficiency comparisons of candidate materials at flight temperature.[3–7] Recently, coefficients have been calculated using both arcjet data and data obtained in a laboratory diffusion reactor to define the surface catalytic efficiency of several materials.[8] Arcjet measurements are limited to surface temperatures in excess of 1100 K and diffusion reactor measurements are required for measurements at lower temperatures. Arrhenius expressions for the recombination coefficients, derived from the temperature-dependent data, are used in computational thermochemistry codes that predict surface heating rates for the real flight case. To predict the full envelope of surface heating rates, atom recombination coefficients are required for surface temperatures ranging from near room temperature to ~1800 K. To determine the catalytic behavior of thermal protection systems at low surface temperatures, a versatile diffusion/flow reactor has been developed that incorporates laser-based diagnostics. This laser diagnostic method alleviates the experimental limitations associated with previous reactor studies that use thermocouple probes to monitor atom concentrations.

A number of laboratory reactor designs have been used to study surface catalysis on materials of low catalytic efficiency such as quartz, Vycor®, Pyrex®, and reaction cured glass (RCG) (Refs. 8–15). Diffusion reactors are particularly well suited for the study of materials of low catalytic activity (i.e., $\gamma < 10^{-2}$). In a diffusion reactor, an rf or microwave discharge dissociates the parent molecule to create atoms. The atoms diffuse down a tube where they can recombine on the walls that are coated with a material of interest and quickly reach a steady-state condition. In some reactor designs atoms may also recombine on a traveling thermocouple probe placed at the center of the diffusion tube. This recombination raises the probe temperature by an amount ΔT. The temperature rise on the probe is measured as a function of distance from the atom source and gives a measure of the atom loss due to wall recombination down the diffusion tube. At proper experimental conditions and within the assumptions of the reactor model, the coefficient γ can be determined from the slope of the line generated in a plot of $\ell n(\Delta T)$ vs X/r.[15]

For studies of low γ materials it is essential to carry out experiments at low pressure (<0.2 torr) to avoid competition between homogeneous and heterogeneous recombination processes.[15] At pressures below ~0.3 torr, diffusion effects are significant, therefore, in a flow reactor, diffusion and convection need to be taken into account. It is simpler to use a dif-

Received July 10, 1995; revision received Oct. 6, 1995; accepted for publication Oct. 6, 1995.

*Senior Research Scientist, Thermal Protection Materials and Systems Branch, Thermosciences Institute.
†Senior Chemical Physicist, Molecular Physics Laboratory.

fusion design alone for reactor modeling. This is the reason for choosing to make γ measurements in a diffusion reactor as opposed to a flow system. The reactor used for this work has been designed for versatility. It is used in the diffusion mode for making γ measurements and in the flow mode when doing titration to determine absolute O- and N-atom concentrations and detection system calibrations.

Most of the previous work in diffusion reactors has been limited to studies of simple first-order surface reactions involving H-, O-, or N-atom recombination because of the lack of species selectivity of the thermocouple probe used for atom detection. The reactor used in the present development is similar, but as an alternative to the thermocouple, applies two-photon laser-induced fluorescence (LIF) to study the effects of atom/surface interactions on catalytic material. LIF offers several advantages over previous detection methods including the nonintrusive nature of the technique that eliminates probe interference with the flowfield, contamination of the reactor from the metal surfaces, and instability of the thermocouple. The technique is species selective, so that, in many cases related to spacecraft entry, the reactant and product concentrations can be monitored directly. Systems containing two or more atomic species can also be investigated. Because of these features, the study of more complex reactions such as $N + O \rightarrow NO$ (there is little data currently available on this surface catalyzed reaction) or $CO + O \rightarrow CO_2$ (which is an important issue for entry into the Martian atmosphere), is feasible. Although more involved than relative measurements, LIF is used often for absolute concentration measurements that are essential for determination of second-order or more complex reaction systems.

This article describes the design, operation, calibration, and integration of the two-photon LIF detection methods into the well-established diffusion reactor approach to evaluate its unique attributes to test the reactor models. The state specificity and high spatial resolution are exploited to examine the O-atom fine-structure equilibrium and to study radial population distributions. Many of the experimental complications involved in measuring atom recombination coefficients by this method have been identified, evaluated, and minimized in these preliminary investigations. The application of LIF presented here focuses on room temperature detection of O and N atoms generated by a microwave discharge in a diffusion/flow apparatus. A quartz surface is chosen for measurements to compare and evaluate the detection methods because the surface is fairly well defined and atom recombination on quartz has been well studied.[9-15] The material is also readily available and optically transparent. In addition, quartz is expected to behave similarly to RCG, which consists primarily of silica.[16] This evaluation is critical in establishing a design for an improved, temperature controlled diffusion reactor for future surface catalysis investigations.

Experimental Approach

Reactor Description

The reactor design is based on a modification of the simple design first introduced by Smith in 1943.[15] A schematic diagram of the reactor is shown in Fig. 1. The main body of the reactor is a quartz cross with 28-cm-long arms in the primary flow direction and two quarter-in. gas inlet ports located 3 and 6 cm upstream of the cross. The o.d. of the primary tube is 25 mm. The gases to be discharged enter this tube after flowing through calibrated mass flow meters permitting the determination of the partial pressures of stable species from a measurement of the total gas pressures and the individual flows. The tube is exhausted through a flexible vacuum hose and a valve attached to the pumping system. The pumping line is refrigerated close to the roughing pump to minimize backstreaming of pump oil into the reactor. The system base pressure is 10–20 mtorr. On one side of the cross is a quartz tee. One connection on the tee is used for a quartz window to allow for the exit of the laser beam from the diffusion side arm and the second port is used for a 10-torr capacitance manometer pressure gauge to monitor the total pressure in the reactor. The diffusion side arm (80 cm long) is attached to the last remaining port on the cross. At the end of this diffusion tube is a

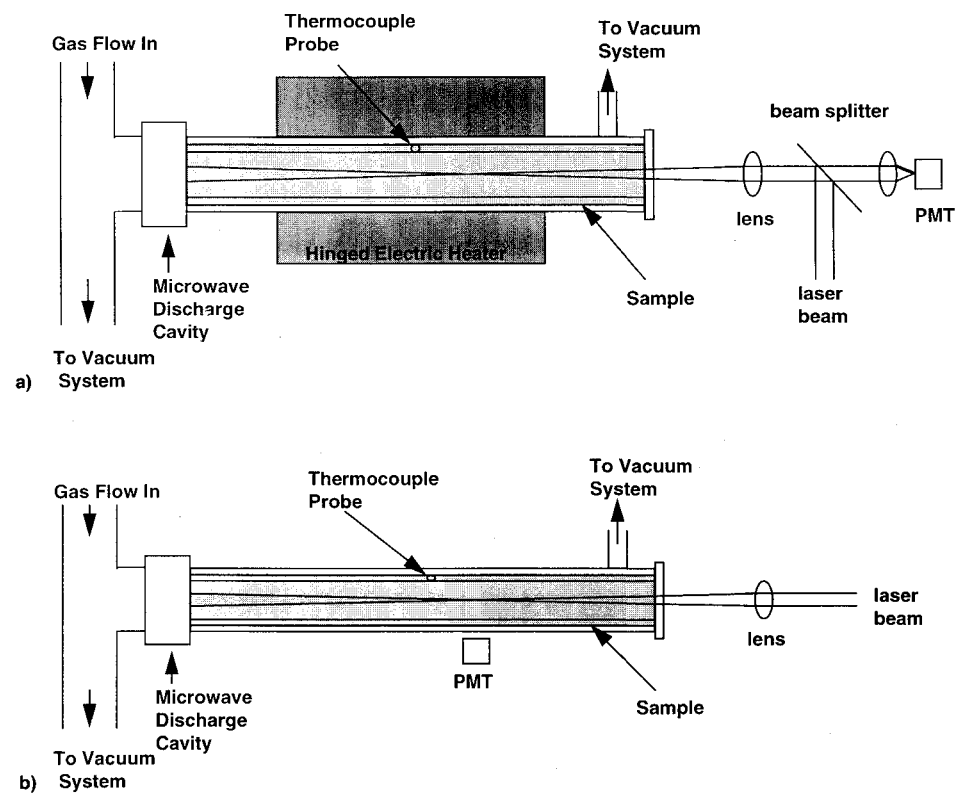

Fig. 1 Schematic diagram of diffusion reactor experimental apparatus: a) on axis and b) perpendicular fluorescence detection.

removable quartz window for entry of the laser beam axially down the tube and a port to evacuate the tube when it is used as a flow tube. By the opening and closing of two valves the diffusion reactor can be transformed into a flow reactor with the entire flow of gas passing through the diffusion side arm. The reactor is mounted on a track to translate the reactor relative to the position of the focal point of the detection laser beam to obtain concentration profiles of the detected species down the diffusion side arm. The system can be equipped with a furnace as shown in Fig. 1a for temperature-dependent γ measurements. The furnace is not used for these initial investigations and all of the experiments are performed at room temperature.

Active species are generated in a microwave discharge. A 2.5-cm-diam microwave cavity can be mounted in the system at several positions. Experiments are performed with the cavity attached on the diffusion side arm and also on the upstream end on the primary flow tube. In the latter configuration other gases can be added to the discharge products to reactively generate atomic species or titrate the atoms to obtain absolute concentrations. Power is applied to the cavity through a double stub tuner from a 100-W microwave power supply. The microwave cavity is forced air cooled.

Atom LIF Detection

Two-photon LIF is used for detection of ground state O and N atoms.[17-22] The energy level diagrams in Fig. 2 show the detection scheme for these processes. For the O-atom case, tunable uv laser radiation near 226 nm excites O atoms from a specific fine-structure component of the $2p\ ^3P_{J''}$ ground state to the $3p\ ^3P_{J'}$ state (J'' and J' can equal 0, 1, or 2). After this initial excitation, fluorescence to the $3s\ ^3S$ state near 845 nm is monitored. The excited $3p\ ^3P$ atom radiative lifetime is about 35 ns.[19] For the N atoms, laser radiation near 211 nm excites N atoms from the $2p^3\ ^4S^0$ ground state to any of the four fine-structure components of the $2p^23p\ ^4D^0$ state. After excitation, the N atoms will fluoresce near 870 nm to the $2p^23s\ ^4P$ state. The radiative lifetime of the $^4D^0$ state is about 43 ns.[20]

In both atoms the intensity of the fluorescence signal (I = photons per laser pulse) is directly proportional to the population in the ground state times a fluorescence efficiency factor. The fluorescence efficiency factor or fluorescence quantum yield is reduced from a maximum value of 1 by collisional quenching that is sensitive to temperature, gas composition, and pressure. In these experiments, the density of atoms relative to the density of efficient quenchers (diatomics) is low so that atom concentration changes along the diffusion tube are not expected to influence the quenching rates.[20,22] The fluorescence intensity, after making corrections for collisional quenching, can be used to extract the atom concentration. Because both O- and N-atom LIF are two-photon processes, most of the signal comes from the area near the focus of the excitation laser beam and, therefore, the atom concentration can be measured at various positions in the diffusion reactor by either moving the reactor or moving the focus of the laser beam and the detector. A combination of the laser beam geometry and the optical characteristics of the fluorescence detection system determines the spatial resolution of the detection method.

In this study, a Lambda Physik excimer pumped dye laser (EMG 102, LPD 3002) generates tunable blue light between 420–460 nm. The laser output is frequency doubled in a β barium borate crystal to generate light near the atom two-photon transitions (226 and 211 nm). The dye laser fundamental and the doubled light are separated using either a Pellin–Broca prism or dichroic mirrors and the uv light is directed into the diffusion reactor. The power of the uv laser light is monitored using a joulemeter (Gentec) interfaced into a gated integrator (SRS). A red sensitive photomultiplier tube (PMT, R666) detects the fluorescence. A colored glass and an interference filter select only the wavelength region near 840–880 nm for detection. The output of the PMT is amplified and the signal is extracted using a gated integrator. The fluorescence and laser power signals are both monitored by a computer and stored for analysis.

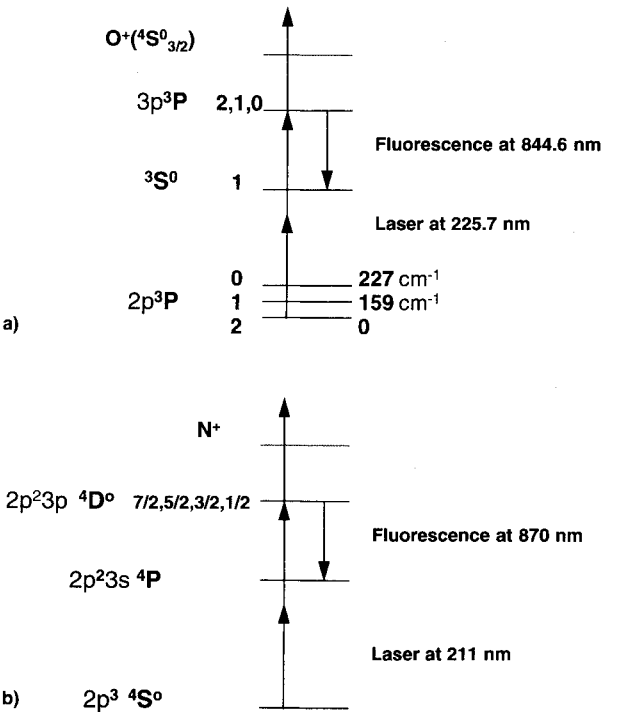

Fig. 2 Energy level diagrams depicting the two-photon fluorescence detection schemes for a) O and b) N atoms.

Fluorescence measurements are made on axis (Fig. 1a) as well as by detection at right angles to the incident laser (Fig. 1b). With the axial fluorescence collection geometry, the signal can be obtained from regions that have limited optical access. The right angle fluorescence measurements are not possible with the furnace in place. In future high-temperature experiments where the furnace is permanently installed, the entire fluorescence detection system, rather than the reactor, will be mounted on a translation stage.

LIF Technique Diagnostics

Several preliminary experiments are required prior to the measurement of the atom signal profiles down the diffusion tube. Laser fluence [f_L (photons cm^{-2} s^{-1})] effects must be studied and the LIF detection system evaluated. Measurements of the laser fluence dependence are useful in the selection of optimum conditions for LIF such as lens focal lengths and geometry of collection optics. If the laser fluence is too high, several processes can interfere with accurate concentration determination by causing a decrease in the fluorescence intensity. These include generation of amplified spontaneous emission (ASE, Ref. 23) and saturation of the two-photon transition. Absorption of a third photon may occur which, for atom detection, will cause photoionization and loss of a fluorescent photon. Two-photon photodissociation of O_2 (Ref. 24) and one-photon dissociation of vibrationally excited species[25,26] have been reported to influence fluorescence intensity during O-atom detection. Ideally, for two-photon atom detection by LIF the fluence dependence of I will be proportional to f_L^n, where $n = 2$. A log–log plot of I vs the laser fluence yielding $n \neq 2$ is a clear indication that processes other than two-photon fluorescence are having a significant influence on the fluorescence intensities. These, at times, undesirable effects will be significant at high laser fluence and can be minimized or eliminated by using lower pulse energy and softer focusing of the laser beam. Changing the focusing and pulse energy changes the spatial extent of the LIF in a complicated manner[27] and

will affect the spatial resolution of the method. The detection system can be designed to compensate for changes in the laser characteristics. For these measurements we must evaluate if a laser fluence squared normalization is appropriate for the experimental data. Absolute measurements require both knowledge of the laser fluence and also confirmation that the signal shows a two-photon dependence. Requirements for the relative measurements reported herein are less restrictive. If the fluence is not constant throughout a measurement, some guidelines must be established on how changes will affect the signal.

Figure 3 shows a log plot of the N-atom signal vs the laser pulse energy in microjoules that is proportional to laser fluence for a given beam geometry. The circles correspond to the N-atom signal. The N-atom signal increases with increasing pulse energy. The data are normalized at 65 μJ. The solid line is the energy dependence for a linear dependence on energy and the dashed line for the anticipated energy squared dependence. Clearly, the N-atom signal is between the two limits and is neither linear nor quadratic in the pulse energy. At low energies (<20 μJ) the slope approaches the two-photon dashed line. Clearly, phenomena such as ionization are occurring at the higher pulse energies. However, since absolute concentration measurements are not required in this case the laser is operated in the 40–70-μJ energy region with a 40-cm lens where the absolute signals are larger. The O-atom fluorescence data show similar behavior and there is no evidence for O_2 photodissociation processes as mentioned earlier. Because of this complicated dependence, pulse energy normalization is not straightforward and in all of the profile measurements the laser pulse energy is maintained at a nearly constant value. Long-term decreases in laser pulse energy are monitored and measurements are repeated to account for the typical 5–10% changes during a typical run.

Before an atom profile can be measured, the collection efficiency of the optical system must be determined at all positions along the tube axis. The calibration must be made when the atom concentration is constant both across the tube and along the tube diameter. To obtain a uniform distribution of atoms two methods are used. In the first, used only for O atoms, O_3 is allowed to diffuse into the side arm at a total pressure of 2.2 torr. O atoms are produced by laser-induced dissociation of O_3 at various axial positions in the tube and, within the same laser pulse, O atoms are probed via LIF. In the O_3 calibration data, the signal appears to be relatively flat along the center of the tube and no collection efficiency correction to the atom loss data is necessary for axial profiles. The diffusion side arm is also converted into a flow tube by changing the flow of the gases in the system. Under typical experimental conditions, the flow rates for the precursor species varies between 20–80 sccm that generates pressures between 0.2–0.5 torr. Reaction of O and N atoms with the walls is negligible under these conditions. Constant values (±10%) of the atom signal are obtained over the entire length of the tube for both O and N atoms. It is therefore concluded that no correction need be applied to the atom concentration profiles in the axial direction.

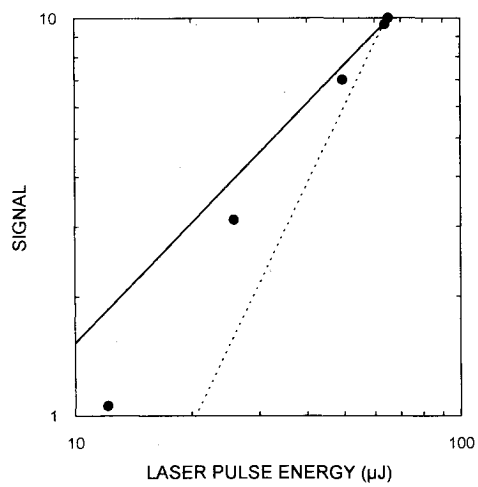

Fig. 3 LIF signal intensity vs laser pulse energy for N-atom detection. The circles correspond to the N-atom signal. The solid line represents a linear energy dependence for the LIF signal and the dashed line represents the anticipated energy squared dependence.

Measurement of Atom Concentration Profiles

Concentration profiles are obtained by scanning the vacuum apparatus relative to the two-photon LIF region. The signal at a given position is measured by recording the averaged output of the gated integrator on a computer for between 50–150 s. The laser is then blocked and the apparatus is moved to another position where the laser is unblocked. Observations typically begin about 5 cm from the center of the discharge cavity and extend for 25 cm when using the 40-cm lens. Depending on the number of positions, this procedure can last for between 10–30 min per discharge condition. Often the first data point is repeated at the end of the scan to verify the long-term stability of the signal. Later, the signal is averaged over the region of exposure to obtain the experimental value. Each position

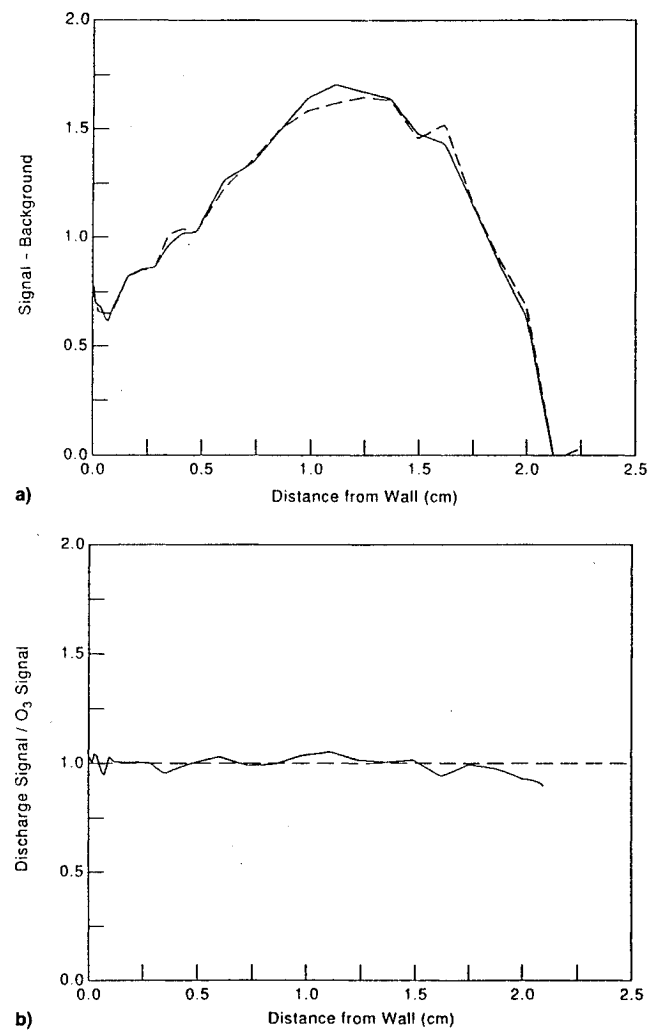

Fig. 4 Radial distribution profiles in diffusion reactor (LIF signal intensity vs radial position in side arm): a) discharge vs O_3 signals, the laser beam propagates down the tube at a small angle to get close to the wall. The abrupt cutoff near 2 cm is caused by the beam being cut off at the entrance to the diffusion side arm and b) radial profile using O_3 calibration. ——, discharge and – – –, O_3.

results in a point on a graph as shown in Fig. 4. If significant differences are observed between the initial and final point taken at the same position, a linear correction for this change in signal is applied to all the experimental data. This correction is typically between 5–15% and is caused by a decrease in the laser power with time.

Results

Atom concentration decays are measured under many different conditions and experimental setups. These include changing the total pressure in the system, changing atom concentration, method of atom preparation, and surface conditions. For both the N- and O-atom experiments standard operating conditions are established as a method for comparison of surface properties from day-to-day. For N atoms, the standard conditions are a 30-W N_2 discharge located on the diffusion side arm at a total pressure of between 0.29–0.31 torr. For O atoms, the standard operating conditions are a 40-W discharge in 0.19–0.21 torr of a pure O_2 on the side arm. Small changes in laser power, microwave power, and alignment influence the magnitude of the signal, but should not alter the signal decrease down the tube. To parameterize the data, the atom decay is fit by extracting the slope μ from a plot of the natural logarithm of the signal vs the distance from the center of the discharge divided by the radius of the tube. For an individual atom signal profile measurement the average uncertainty (two standard deviation) in μ is about 9% for N atoms and 10% for O atoms. The results of the measurements are presented in Table 1. For N atoms the day-to-day reproducibility is excellent and very little difference is seen between the uncertainty in an individual slope (9%) and the uncertainty in the average of all the measurements (11%). For O atoms there is a doubling in the uncertainty of the average (22%) over that of an individual run (10%). This may be due to changes in the surface properties from day-to-day that effect the O-atom signal decay. Effects of surface contamination will be discussed later.

Table 1 also presents data obtained when the microwave discharge is located on the flowing portion of the apparatus. Changing the location of the microwave cavity on the apparatus is required to add gases to the flowing atom stream. Initially, no change was expected in the slope with this experimental configuration, and only a change in the magnitude of the signal due to reaction on the walls prior to the observation region was expected. For O atoms no difference is found in the slope even though the signal size decreases by about a factor of 5. For N atoms, however, the slope is found to be at least a factor of 2 less steep. This is significantly outside the respective errors of the two measurements and indicates that an unexpected process may be occurring. The signal for the N atom case decreases by about an order of magnitude upon moving the discharge. A significant change in the slope that is a function of atom concentration, could indicate non-first-order reaction kinetics. Further study is required to determine if this reduction in the slope is due to the decrease in the N-atom concentration, impurities in the N_2 gas, or changes in boundary conditions that must be accounted for in the reactor model. Without the added sensitivity of the LIF detection method such order of magnitude changes in the N-atom concentration could not be studied.

One factor that must be carefully addressed in these studies is the electronic states of the detected atomic species. For N atoms the lowest lying electronic state is not split and consists of only a single level, but for O atoms the ground state is split by spin–orbit coupling and consists of a fivefold degenerate $J = 2$ level, a threefold degenerate $J = 1$ level, and a $J = 0$ level. The separation is large enough that only a single level is probed by the two-photon LIF process. When in thermal equilibrium the decay of each level down the diffusion tube would be identical, but this has not been considered previously. Since this specific complication is unique to O atoms the discharge preparation will be discussed in more detail.

A discharge generated in a pure O_2 gas may contain vibrationally and electronically excited states of O, O_2, and O_3 as well as ionic species depending on the discharge conditions. Only ground state O atoms are of interest in recombination studies related to the spacecraft re-entry problem. Using LIF, we can detect O-atom loss without interference from O_2, O_3 ground, or vibrationally excited state species. However, the ground state $J = 2$ population of O atoms measured will be affected by collision-induced quenching of electronically excited O atoms and by variations in the J-level population in the ground state. Previous work[14] indicates that excited electronic states are completely quenched within five radii of the center of the discharge at the pressures used in these experiments (~0.2 torr).

Ideally, the rate of loss of O atoms measured from any of the ground state J levels would yield the same slope if a constant temperature equilibrium distribution exists. In an experiment to test this hypothesis, the laser is scanned over the three fine structure components at several axial positions of the discharge tube. The area under the peaks is then obtained through integration of the spectra. The results for the slope of the removal for each ground state level are 0.043 ± 0.006, 0.026 ± 0.011, and 0.036 ± 0.009 for $J = 0$, $J = 1$, and $J = 2$, respectively. This unexpected result indicates that either the temperature is not constant over the region of measurement or that the fine structure levels are not in equilibrium. If it is assumed that a thermal equilibrium distribution at 300 K is present 30 cm from the discharge, then the percentage of the total ground state population in each level is 5, 21, and 74% for $J = 0$, 1, and 2, respectively. Given the measured slopes of the fine structure removal measurements at 10 cm from the discharge, the relative populations are 6, 18, and 76% for $J = 0$, 1, and 2, respectively. At first glance this appears to be a small difference, however, for the two levels that are least populated at room temperature the slope change is significant. From these results, the data obtained from the $J = 2$ level will be most reliable in making atom loss measurements and that level also produces the largest signal. The change in the distribution will produce only a few percent change in the slope for $J = 2$. All of the O-atom measurements described previously are made using the $J = 2$ level. It is possible that the microwave discharge process itself may generate a nonthermal distribution over fine structure states. Also, collisional and radiative relaxation of higher lying electronic states may account for part of this distribution. Further experiments are required to determine the source of this difference between the fine-structure components.

Table 1 Atom signal profiles for standard conditions and different discharge positions

Atom	Discharge position	Number of measurements	Range of slopes	Average slope
O	Sidearm	6	0.036–0.046	0.041 ± 0.009
N	Sidearm	7	0.043–0.050	0.046 ± 0.005
O	Flowarm	4	0.037–0.050	0.041 ± 0.010
N	Flowarm	7	0.018–0.022	0.021 ± 0.002

Table 2 O and N-atom recombination coefficients on quartz obtained at room temperature at different pressures

Atoms	P, torr	μ	γ, $\times 10^5$
O	0.2	-0.042 ± 0.006	7.1 ± 2.2
	0.4	-0.057 ± 0.003	6.3 ± 0.7
	0.5	-0.089 ± 0.003	12.6 ± 0.9
	0.7	-0.104 ± 0.004	13.0 ± 1.1
N	0.2	-0.043 ± 0.003	6.9 ± 0.5
	0.3	-0.047 ± 0.004	5.5 ± 0.9
	0.5	-0.055 ± 0.001	4.5 ± 0.1
	0.8	-0.082 ± 0.003	6.3 ± 0.5

In a last set of experiments the total pressure in the system is varied. This provides a critical test of the extraction of the surface recombination coefficient γ from the removal slope μ. Table 2 summarizes the results at different total pressure for both O and N atoms. The extraction of γ from these measurements is described next.

Determination of Atom Recombination Coefficients from Atom Loss Data

Atom recombination coefficients γ can be extracted directly from the atom loss as a function of distance from the microwave discharge cavity. For a reaction that is first order with respect to the gas phase atom concentration, γ can be calculated from the following expression, which is derived in detail for diffusion in a cylindrical tube in Refs. 14 and 15:

$$\gamma = 2\mu^2 D/vr \tag{1}$$

The additional factor of 2 in Eq. (1) is included because two atoms are lost from the gas phase for formation of each O_2 molecule (one is needed to replenish the active site on the surface).

A simple expression for the diffusion coefficient was empirically derived from the Chapman–Enskog equation using values of collision cross sections obtained from Ref. 28:

$$D = D_0(T/T_0)^{1.64}(P_0/P) \tag{2}$$

D_0 is the diffusion coefficient at room temperature ($T_0 = 298$ K) and atmospheric pressure ($P_0 = 760$ torr). At standard temperature and pressure $D_0 = 0.365$ cm^2 s^{-1} for O atoms in O_2 and $D_0 = 0.364$ cm^2 s^{-1} for N atoms in N_2.

Equation (1) is derived from a model that assumes that the surface recombination is first order with respect to the gas phase atom concentration. To ensure that the model correctly describes the experimental data, the experimental conditions must be properly controlled. As mentioned previously, the reactor is not used in flow mode for γ measurements because the coefficients for the materials of interest are very small. The pressure in the reactor should be kept near or below 0.2–0.3 torr to avoid gas phase recombination resulting from three body collisions.[15] At higher pressures, wall recombination competes with gas phase recombination and atom loss rates are not representative of heterogeneous catalysis alone. For work done at higher temperatures, it may be possible to use a flow reactor because gas phase recombination drops dramatically as temperature increases.[29] There is too much uncertainty in the data currently available in the literature on three-body recombination to determine at what temperature these gas phase processes can be ignored.

The intensity of the LIF signal is measured as a function of distance from the discharge and gives a measure of the atom loss down the diffusion tube. For a first-order reaction, the atom recombination coefficient can be determined from the slope of the line generated from a log plot of LIF signal intensity vs distance from the discharge. The model used to calculate recombination coefficients from experimental data was developed by Smith.[15] This model makes the following assumptions:

1) There is no radial concentration distribution ($\gamma < 10^{-2}$).

2) Atom loss is due primarily to heterogeneous catalysis (pressure is low enough to avoid gas phase recombination).

3) The diffusion tube is long enough that end effects are negligible.

4) Temperature is constant along the tube where measurements are made to avoid variations in diffusion effects and recombination rates.

These issues must also be considered when making comparisons of γ values found in the literature. (Note that values of γ found in the literature that are $>10^{-2}$ are suspect if measured by the diffusion reactor method and no radial distribution measurements have been made. Also, γ values determined through surface temperature or heat flux measurements may be susceptible to errors because the surface energy accommodation coefficient is not always equal to 1.) To make reliable measurements of γ by this method, it is necessary to examine all possible sources of experimental error that could affect these assumptions.

Literature values of γ for O atoms on silica and some metals may vary by up to several orders of magnitude for any number of reasons. Much of the information necessary to make comparisons is often not made available (such as how γ was calculated). It should be made clear that many of the recombination coefficients reported in the literature are not absolute values, but apparent γ values ($\gamma = \gamma_{absolute} F_{roughness}$). (Also note that γ values measured from O atom loss are a factor of 2 larger than those measured from detection techniques that monitor O_2 formation.) A surface roughness measurement is necessary to calculate the absolute values that are necessary for determination of many of the physical properties of the surface.[14] In our work, apparent γ values are useful to determine the relative catalytic activity between materials, but absolute values would provide more physical insight into the actual recombination processes. Methods of making roughness measurements on thermal protection system (TPS) surfaces are currently under investigation.

Without careful consideration, three main aspects of the experiment could lead to large errors or misinterpretation of atom loss data. These include 1) sample surface properties, 2) reactive gas pressure and composition, and 3) reactor design. These issues will be discussed independently as they relate to the experimental model previously outlined.

Sample Surface Properties

Surface catalytic activity. Low surface catalytic activity ($\gamma < 10^{-2}$) is important for reliable measurements using the current reactor model. If the reaction rate at the surface is too high, a radial distribution will develop in the reactor. The current model assumes a uniform concentration distribution across the tube diameter at all axial locations in the tube. It is important to ensure that either there is no radial distribution or that the reactor model is modified to account for radial distributions. In either case, radial concentration distributions can be measured experimentally by LIF detection. Using LIF, radial distributions can be measured with $\leq$200-μm resolution by measurement of fluorescence intensity as a function of laser beam position along the diameter of the tube. In this work the exact radial size was not measured, but from the rapid fall of the signal shown in Fig. 4, reasonable upper limits can be obtained. The axial resolution of 1 cm was determined experimentally via the rapid decrease in the signal at very high pressure. An experimental measurement of axial resolution is preferred over a calculated value since many nonlinear processes can affect this value.[27]

For measurements of radial concentration profiles, the PMT is mounted at a right angle to the input beam and detects the fluorescence passing through the quartz sample. This configuration gives larger signals than the on-axis detection, resulting

in more accurate radial profiles. The dichroic mirror is replaced by a prism and this prism and the focusing lens are mounted on a translation stage that could be scanned perpendicular to the tube. Because of the nonuniformity along the tube and the focusing of the beam, the only way to bring the laser beam close to the wall at the focus was to have the propagation direction of the laser beam and the axis of the tube at a small angle.

Before making measurements of radial distribution the collection efficiency of the optical system across the tube diameter is determined, as described previously. The ozone is studied in both the diffusion and flow mode and no difference in radial distribution is seen between the two conditions. Data are obtained in a similar experiment where O atoms are generated in the microwave discharge and have diffused 5 cm down the tube. In this case wall reactions may influence the radial distribution. The normalized radial distribution is similar to the calibration distribution, as expected under these experimental conditions. Figure 4a shows a comparison of the scattered light subtracted signals for O atoms produced in the discharge in the diffusion mode and the ozone calibration in the flowing mode. In both cases, the signal appears to be relatively flat in the center of the tube and drops near the walls due to a decrease in collection efficiency. No significant difference is seen between this and the O_3 calibration profile. Figure 4b illustrates this similarity by dividing the O-atom signal by the ozone signal. Only scatter is seen about the expected value of one and no systematic trends are observed. This should be the case for low γ materials such as quartz at $P \sim 0.2$ torr where the diffusion coefficients are relatively high. Any depletion of O atoms due to wall reactions is rapidly compensated for through rapid diffusion. Radial profiles are obtained in flow and diffusion modes at several pressures, pumping speeds, and distances from the discharge. All show similar profiles independent of the mode of operation.

Under the conditions of this study no radial distribution is expected because of the low recombination at the surface, but this study demonstrates that two-photon LIF will be extremely useful for studying any radial distribution effects in other systems and would be invaluable for development of reactor models for higher γ materials studied in the same apparatus.

Sample surface composition. To test the feasibility of the experimental methods, most experiments are performed at room temperature with a quartz surface observing the fluorescence at right angles to the laser beam through the tube walls. Measurements are made after several days of pumping the system to ~2×10^{-2} torr to reduce the presence of water on the quartz walls. Significant surface coverage by water has been shown to reduce the heterogeneous atom recombination probability for N atoms,[14] but not significantly for O atoms.[11] This may account in part for variations in γ values for N-atom recombination found in the literature. It is accepted procedure to heat the sample to ~450°C under vacuum (~10^{-6} torr) to drive off water for more accurate γ_N determinations. Ultrahigh purity gases should also be used to ensure system cleanliness. This is not done in the current work because the goal is not to measure γ accurately, but to understand how γ varies with experimental conditions to demonstrate the capabilities of the laser detection method and test the reactor model. Therefore, it is assumed that the average γ_O and γ_N values (~8×10^{-5} and 6×10^{-5}, respectively) are those for a quartz surface with some water and possible organic contamination. In this work, heating the surface and pumping on the system does not significantly affect γ for N atoms.

To demonstrate that major effects can result from minor contaminants, γ for O atoms is measured after introducing small amounts of NO into the system while the total O_2 pressure is ~0.22 torr. The atom loss data was obtained as the NO partial pressure was changed from 0 to 1%. The corresponding γ_O value is reduced from $6(\pm 1.0) \times 10^{-5}$ to $3(\pm 0.3) \times 10^{-5}$ to $4(\pm 0.3) \times 10^{-6}$ for 0, 0.3, and 1% added NO, respectively. This behavior is expected because the surface becomes poisoned with NO, which reduces the number of available reaction sites for the O-atom recombination.

The γ_O values (Table 1) obtained at pressures near 0.2 torr over an approximately four-month period were reproducible to within a factor of 2. This is very reasonable for room temperature measurements considering no special efforts were taken to purify gases or ensure that pump oil vapors were not condensing on the wall of the reactor. It has been noted in previous work by other methods[14] that γ values obtained at room temperature in a single laboratory may vary by a factor of 4 and those obtained in different laboratories may vary by several orders of magnitude. It is expected that the reproducibility will improve with increasing temperature and will be good even at low temperatures when proper precautions are taken to ensure system cleanliness.

Reactive Gas Properties

Total pressure dependence. Changing the pressure of the O_2 or N_2 in the reactor will have an effect on the atom loss rate through the diffusion tube. This can be caused by changes in the diffusion rate with pressure, homogeneous reactions enhanced at higher pressures, an increase or decrease in the atom concentration, or other as yet uncharacterized phenomena. As a result, changing the total system pressure tests the system models and our understanding of the details of the atom loss.

Figure 5a shows the data obtained in an experiment where O atoms are generated in the microwave discharge at a total pressure of 0.22, 0.41, and 0.67 torr of pure O_2. Figure 5b

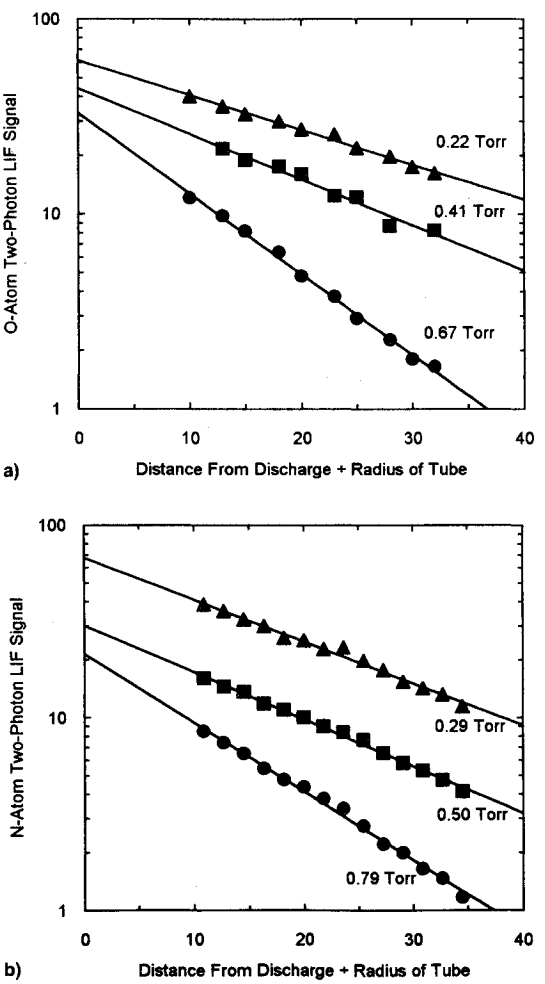

Fig. 5 LOG (LIF signal intensity) vs distance from discharge as a function of total system pressure: a) oxygen and b) nitrogen atom decay curves.

displays the results of a similar experiment with N atoms. If we assume that recombination on the reactor walls is the only mechanism for atom loss, the different slopes observed in the atom loss data should be due only to differences in diffusion coefficient and the resulting γ values should be the same for all three cases. The diffusion coefficients at 0.22, 0.41, and 0.67 torr are 1261, 677, and 414 $cm^2\ s^{-1}$, respectively. The γ value calculated from Eq. (1) is the same (within experimental error) at 0.22 and 0.41 torr and increases by a factor of 2 at 0.67 torr (Table 1). Similar behavior is observed for N atoms in N_2. These findings indicate that at 0.41 torr, there is no significant contribution to atom loss from homogeneous reactions, but the atom loss curves may be affected by reactive three-body collisions in the gas phase at the higher pressure.

At pressures below 1 torr and less than 10% dissociation of the O_2, the most likely homogeneous reactions to affect the atom loss curves are the following:

1) $O + O_2 + O_2 \rightarrow O_3 + O_2$ 1.9×10^{-35} $cm^6\ s^{-1}$ (Ref. 29)
2) $O + O_3 \rightarrow O_2 + O_2$ 2.0×10^{-35} $cm^3\ s^{-1}$ (Ref. 29)
3) $O + O + O_2 \rightarrow O_2 + O_2$ 2×10^{-33} $cm^6\ s^{-1}$ (Refs. 29, 30)

Using this kinetic data, the reactor model predicts that three-body recombination in the gas phase will begin to have an observable influence on the atom loss curves at total system pressures above 0.5 torr for a diffusion tube of 22-mm i.d.

Atom concentration dependence. Measurements of atom loss curves as a function of the partial pressure of reactive species also play an important role in determination of reaction mechanisms. Preliminary experiments involved making measurements of atom loss under a variety of experimental conditions. It should be noted that atom loss due to diffusion into the bulk material will affect atom loss measurements and must be taken into account in the data analysis. This has been demonstrated in Ref. 31 and has been shown not to be a problem in studies of O-atom recombination on reaction cured glass that consists predominantly of silica. Figure 6 shows N atom loss data obtained at a total pressure of ~0.3 torr. The LIF signal intensity I is plotted vs distance from the discharge. These data are obtained in two separate experiments where the microwave discharge was placed in different positions on the side arm. The circles represent data obtained while the discharge was placed in its normal position. The triangles represent data obtained while the discharge was positioned 10 cm further upstream. This allows atom loss data to be collected over larger distances from the atom source, which helped to increase confidence in the exponential fit of the data. An exponential fit to the data indicates that the reaction is first order in N-atom concentration. Further confirmation of the first-order atom recombination process is obtained in studies of O- and N-atom partial pressures. Linear $\ell n(I)$ vs X/r plots are obtained in experiments where the initial N-atom concentration was varied by changing the power of the microwave discharge while the total pressure in the system remained the same. Increasing the initial concentration by up to a factor of 5, at a constant total pressure, gives linear log plots with the same slope within experimental error, independent of concentration. This behavior is characteristic of first-order reactions.

The validity of using a first-order reaction assumption in the calculation of γ for O- and N-atom recombination on silica at moderate and low temperatures has been demonstrated in many previous investigations.[9-15] Detailed descriptions of the temperature-dependent atom recombination on silica are given elsewhere and will only be briefly discussed here. Under steady-state conditions at low temperatures a large fraction of the surface is assumed to be covered with chemisorbed atoms. Recombination occurs when an atom from the gas phase strikes a chemisorbed atom on the surface (Eley–Rideal mechanism). At higher temperatures, thermal desorption reduces the number of reaction sites on the surface, but the reaction remains first order. At some critical temperature related to the binding energy of the chemisorbed species, thermal desorption becomes a dominating process and surface coverage is proportional to the atom concentration in the gas phase. At this point the recombination reverts to a second-order process where two atoms diffusing along the surface must react for recombination to occur (Langmuir–Hinschelwood mechanism). For more detailed discussion of the reaction models see Refs. 14 and 32–34.

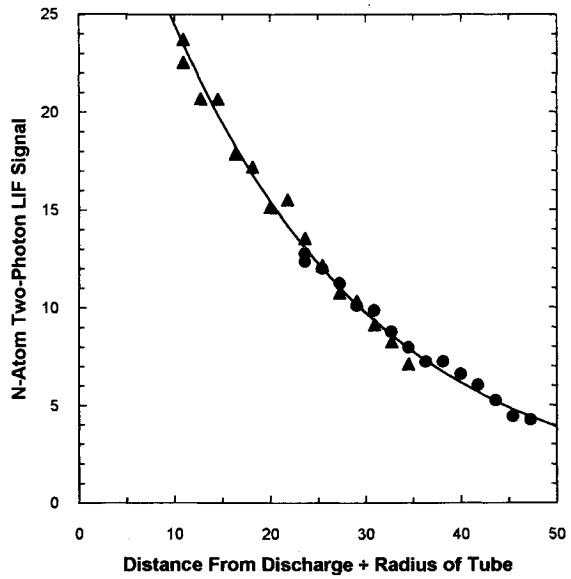

Fig. 6 Exponential fit of N-atom loss curve. LIF signal intensity vs distance from discharge/tube radius over a 30 cm distance at ~0.3 torr. The circles represent data obtained while the discharge was placed in its normal position. The triangles represent data obtained while the discharge was positioned 10 cm further upstream.

Near the critical temperature, the first-order reaction rates should begin to drop rapidly and the reaction should revert to a second-order process. This effect has been observed near 1250 K for N- and O-atom recombination on silica[10,11] and was first observed on a reaction-cured glass during arcjet tests at higher temperatures.[4] These observations lend further support to the assumptions of first-order reaction mechanisms that are made to develop models for proper data analysis. Much more concentration-dependent data is needed in the critical temperature region to better understand the gas surface interactions and develop models that allow analysis of second-order reaction kinetics. This type of data would provide important information for studies of spacecraft TPS, because above the critical temperature, catalytic recombination becomes a less important contributor to re-entry heating.

Effects of Reactor Design

One of the most important assumptions made for the diffusion reactor model is that the diffusion tube is infinitely long, and therefore, tube end effects can be ignored. Since the reactor hardware consists of a tube of finite length, studies must be made to determine how the tube length affects the γ values. If the tube is too short, atoms reaching the end of the tube will be reflected back into the observation region. This will change the atom loss curves and result in lower than expected recombination coefficients unless reflective boundary conditions are included in the reactor model.

Ideally, all atoms would be lost to wall recombination before reaching the end of the tube so that reflective boundary conditions would not need to be included in the reactor model. The problem could be partially alleviated by using a higher total pressure (i.e., 0.5 torr) to decrease the diffusion coefficient thereby reducing the number of atoms reaching the end of the reactor tube. However, at the low pressures used for

most of these experiments (0.3 torr), there is only a factor of 2–3 reduction in signal intensity over the length of the observation region. At ~0.5 torr, the signal drops by a factor of 7–14 over the length of the tube due to the smaller diffusion coefficients at higher pressure. A manuscript is currently in preparation that describes the reactor model in more detail. The model also must account for the effects of metal joints and fittings in the vacuum system that are highly catalytic to atom recombination.

Conclusions

Through this work, it has been established that laser-induced fluorescence provides a versatile and powerful method for detection of O- and N-atom loss in a diffusion tube to measure surface catalytic activity. The experimental apparatus is effective in that it allows fluorescence detection to be used for measuring recombination coefficients and for performing diffusion tube and microwave discharge diagnostics. In spite of the increased complexity of the laser technique it offers many advantages over thermocouple probe methods. With the experience gained in this study and others, LIF methods can be implemented to answer detailed questions in surface catalysis. The measurements can also be made very reliable, reproducible, and routine with the correct equipment and expertise.

The species selectivity of the method has been demonstrated in this work and is currently being used to study the temperature-dependent reaction of N + O to form NO. The reactor design allows the N- to O-atom partial pressure ratio to be reproducibly controlled. This is important because the degree of dissociation of the air in the bow shock of a re-entry vehicle will be temperature dependent. Data will be required over a large range of surface temperatures and atom partial pressures corresponding to a variety of vehicle trajectories.

A great deal of experimental data will be essential to fully understand the catalytic behavior of the numerous thermal protection systems currently available for new vehicle designs. In addition, it is essential to correlate the catalytic data with data obtained from surface chemical analyses. In future work, correlation of diffusion reactor results will be made with data obtained from x-ray diffraction, x-ray fluorescence, x-ray photoelectron spectroscopy, and IR spectroscopy. These analytical techniques will allow observation of chemical changes of surfaces resulting from diffusion, exposure to high temperature, and/or attack by the reactive O and N atoms. Secondary electron microscopy will also be used to correlate surface morphology with catalytic activity. These capabilities will provide detailed information essential to the development of thermal protection materials as well as more accurate recombination data required for improved vehicle designs.

Acknowledgments

This work was funded through NASA's Director's Discretionary Funding Program. Support to J. Pallix under a prime contract to Eloret by NASA, NCC2-14031 is also acknowledged. The authors gratefully acknowledge helpful discussions and assistance in carrying out experiments from David Stewart, Dominic Cagliostro, Kathy Knierim, Marc Onishi, Tom Slanger, and Mark Dyer.

References

[1]Stewart, D. A., Rakich, J. V., and Lanfranco, M. J., "Catalytic Surface Effects Experiment on Space Shuttle," AIAA Paper 81-01143, June 1981.

[2]Stewart, D. A., Rakich, J. V., and Lanfranco, M. J., "Catalytic Surface Effects Space Shuttle Thermal Protection System During Earth Entry Flights STS-2 Through STS-5," *Shuttle Performance: Lessons Learned*, NASA CP2283, Pt. 2, 1983.

[3]Stewart, D. A., Chen, Y. K., and Henline, W. D., "Effect of Non-Equilibrium Flow Chemistry on Surface Heating to AFE," AIAA Paper 91-1373, June 1991.

[4]Kolodziej, P., and Stewart, D. A., "Nitrogen Recombination on High-Temperature Reusable Surface Insulation and the Analysis of Its Effects on Surface Catalysis," AIAA Paper 87-1637, June 1987.

[5]Scott, C. D., "Catalytic Recombination of Nitrogen and Oxygen on High-Temperature Reusable Surface Insulation," *Aerothermodynamics and Planetary Entry*, edited by A. L. Crosbie, Vol. 77, Progress in Astronautics and Aeronautics, AIAA, New York, 1981, pp. 192–212.

[6]Scott, C. D., "Catalytic Recombination of Nitrogen and Oxygen on High-Temperature Reusable Surface Insulation," AIAA Paper 80-1477, July 1980.

[7]Willey, R. J., "Arc Jet Diagnostics Tests, Final Report," NASA-JSC/ASEE SFFP, June 1988.

[8]Stewart, D. A., Pallix, J. P., and Esfahani, L., "Surface Catalytic Efficiency of Candidate Ceramic Thermal Protection Materials for SSTO," Confidential Document TM, CDTM-20007, March 1995.

[9]Krongelb, S., and Strandberg, M. W. P., "Use of Paramagnetic-Resonance Techniques in the Study of Atomic Oxygen Recombination," *Journal of Chemical Physics*, Vol. 31, No. 5, 1959, pp. 1196–1210.

[10]Breen, J., Rosner, D. E., Deglass, W. N., Nordine, P. C., Cibrian, R., and Krishnan, N. G., "Catalysis Study for Space Shuttle Vehicle Thermal Protection Systems," Yale Univ., NASA CR-134124, New Haven, CT, April 1973.

[11]Greaves, J. C., and Linnett, J. W., "Recombination of Atoms at Surfaces, Part 5-Oxygen Atoms at Oxide Surfaces," *Transactions of the Faraday Society*, Vol. 55, No. 8, 1959, pp. 1346–1354.

[12]Linnett, J. W., and Marsdon, D. G. H., "The Kinetics of the Recombination of Oxygen Atoms at a Glass Surface," *Proceedings of the Royal Society of London, Series A: Mathematical and Physical Sciences*, Vol. 234, No. 1199, 1956, pp. 489–504.

[13]Wood, B. J., and Wise, H., "Kinetics of Hydrogen Atom Recombination on Surfaces," *Journal of Physical Chemistry*, Vol. 65, No. 1, 1961, pp. 1976–1983; also Wood, B. J., and Wise, H., "The Interaction of Atoms with Solid Surfaces," *Rarefied Gas Dynamics*, edited by L. Talbot, Academic, New York, 1961, pp. 51–59.

[14]Kim, Y. C., and Boudart, M., "Recombination of O, N, and H Atoms on Silica: Kinetics and Mechanisms," *Langmuir*, Vol. 7, No. 12, 1991, pp. 2999–3005; also Kim, Y. C., "Atom Recombination on Surfaces," Ph.D. Dissertation, Stanford Univ., Stanford, CA, 1991.

[15]Smith, W. V., "The Surface Recombination of H Atoms and OH Radicals," *Journal of Chemical Physics*, Vol. 11, No. 3, 1943, pp. 110–125.

[16]Goldstein, H. E., Leiser, D. G., and Katvala, V., "Reaction Cured Borosilicate Glass Coating for Low-Density Fibrous Silica Insulation," *Borate Glasses*, Plenum, New York, 1978, pp. 623–634.

[17]Bischel, W. K., Perry, B. E., and Crosley, D. R., "Two-Photon Laser-Induced Fluorescence in Oxygen and Nitrogen Atoms," *Chemical Physics Letters*, Vol. 82, No. 1, 1981, pp. 85–88.

[18]Bischel, W. K., Perry, B. E., and Crosley, D. R., "Detection of Fluorescence from O and N Atoms Induced by Two-Photon Absorption," *Applied Optics*, Vol. 21, No. 8, 1982, pp. 1419–1429.

[19]Bamford, D. J., Jusinski, L. E., and Bischel, W. K., "Absolute Two-Photon Absorption and Three-Photon Ionization Cross Sections for Atomic Oxygen," *Physical Review A: General Physics*, Vol. 34, No. 1, 1986, pp. 185–198.

[20]Copeland, R. A., Jefferies, J. B., Hickman, A. P., and Crosley, D. R., "Radiative Lifetime and Quenching of the $3p^4D^0$ State of Atomic Nitrogen," *Journal of Chemical Physics*, Vol. 86, No. 9, 1987, pp. 4876–4884.

[21]Kroll, S., Lundberg, H., Persson, A., and Svanberg, S., "Time-Resolved Laser Spectroscopy of High-Lying States in Neutral Oxygen," *Physical Review Letters*, Vol. 55, No. 3, 1985, pp. 284–287.

[22]Meier, U., Kohse-Hoinghaus, K., and Just, T., "H and O Atom Detection for Combustion Applications: Study of Quenching and Laser Photolysis Effects," *Chemical Physics Letters*, Vol. 126, No. 6, 1986, pp. 567–573; also Dagdigian, P. J., Forch, B. E., and Miziolek, A. W., "Collisional Transfer Between and Quenching of the $3p^3P$ and ^5P States of the Oxygen Atom," *Chemical Physics Letters*, Vol. 148, No. 4, 1988, pp. 299–308.

[23]Westblom, U., Agrup, S., Alden, M., Hertz, H. M., and Goldsmith, J. E. M., "Properties of Laser-Induced Stimulated Emission for Diagnostic Purposes," *Applied Physics B*, Vol. 50, No. 6, 1990, pp. 487–497.

[24]Miziolek, A. W., and DeWilde, M. A., "Multiphoton Photochemical and Collisional Effects During Oxygen-Atom Flame Detection," *Optics Letters*, Vol. 9, No. 9, 1984, pp. 390–392.

[25]Goldsmith, J. E. M., "Photochemical Effects in Two-Photon-Excited Fluorescence Detection of Atomic Oxygen in Flames," *Applied*

Optics, Vol. 26, No. 17, 1987, pp. 3566–3572.

[26]Wysong, I. J., Jefferies, J. B., and Crosley, D. R., "Laser-Induced Fluorescence of $O(3p^3P)$, O_2, and NO near 226 nm: Photolytic Interferences and Simultaneous Excitation in Flames," *Optics Letters*, Vol. 14, No. 15, 1989, pp. 767–769.

[27]Peze, P., Paillous, A., Siffre, J., and Dubreuil, B., "Quantitative Measurements of Oxygen Atom Density Using LIF," *Journal of Physics D: Applied Physics*, Vol. 26, No. 6, 1993, pp. 1622–1629.

[28]Yun, K. S., and Mason, E. A., "Collision Integrals for the Transport Properties of Dissociating Air at High Temperatures," *Physics of Fluids*, Vol. 5, No. 4, 1961, pp. 380–386.

[29]Schofield, K., "An Evaluation of Kinetic Rate Data for Reactions of Neutrals of Atmospheric Interest," *Planetary Space Science*, Vol. 15, No. 4, 1967, pp. 643–670.

[30]Campbell, I. M., and Gray, C. N., "Rate Constants for $O(^3P)$ Recombination and Association with $N(^4S)$," *Chemical Physics Letters*, Vol. 18, No. 4, 1973, pp. 607–609.

[31]Carleton, K. L., and Marinelli, W. J., "Spacecraft Thermal Energy Accommodation from Atomic Recombination," *Journal of Thermophysics and Heat Transfer*, Vol. 6, No. 4, 1992, pp. 650–655.

[32]Jumper, E. J., and Seward, W. A., "Model for Oxygen Recombination on Reaction-Cured Glass," *Journal of Thermophysics and Heat Transfer*, Vol. 8, No. 3, 1994, pp. 460–465.

[33]Willey, R. J., "Comparison of Kinetic Models for Atom Recombination on High-Temperature Reusable Surface Insulation," *Journal of Thermophysics and Heat Transfer*, Vol. 7, No. 1, 1993, pp. 55–62.

[34]Gelb, A., and Kim, S. K., "Theory of Atomic Recombination on Surfaces," *Journal of Chemical Physics*, Vol. 55, No. 10, 1971, pp. 4935–4939.